Photochemical & Photobiological Sciences (2023) 22:2725–2734
https://doi.org/10.1007/s43630-023-00482-6

ORIGINAL PAPERS

Photodegradation of free base and zinc porphyrins in the presence and absence of oxygen

Barbara Golec[1,2] · Joanna Buczyńska[2] · Krzysztof Nawara[1,2] · Aleksander Gorski[2] · Jacek Waluk[1,2]

Received: 5 May 2023 / Accepted: 7 September 2023 / Published online: 29 September 2023

Abstract

Comparison of photostability in degassed and aerated toluene solutions is reported for 5,10,15,20-tetraphenylporphyrin, 5,10,15-tri(*p*-tolyl)porphyrin, and their zinc analogues. After degassing, quantum yields of photodegradation are higher, but the photodecomposition rates decrease. Lower stability in deoxygenated solutions is due to much longer triplet lifetimes: 200–300 microseconds, compared to 200–360 ns in non-degassed toluene. For the zinc porphyrins, the LC–MS results show that the initial photoproduct contains two oxygen atoms. Based on electronic absorption and calculations, it is assigned to dehydrated zinc biladienone structure, relatively stable in toluene, but readily demetallated in dichloromethane. A similar species is formed also in the case of free bases, but it then undergoes hydration due to traces of water present in the solvent. Zinc derivatives were found to form biladienones even in degassed solutions. To explain this observation, we postulate formation of a complex with remaining oxygen or oxygen-containing species which is not removed by freeze–thaw procedure. This hypothesis is confirmed by MS results and by the analysis of photodegradation products obtained when zinc porphyrin is complexed with dimethylsulfoxide (DMSO). Under these circumstances, changes in absorption are the same as in the absence of DMSO when non-degassed toluene is used, but irradiation of deoxygenated solutions leads to a different photoproduct. For both degassed and non-degassed solvents, complexation with DMSO results in the enhancement of photostability.

Graphical abstract

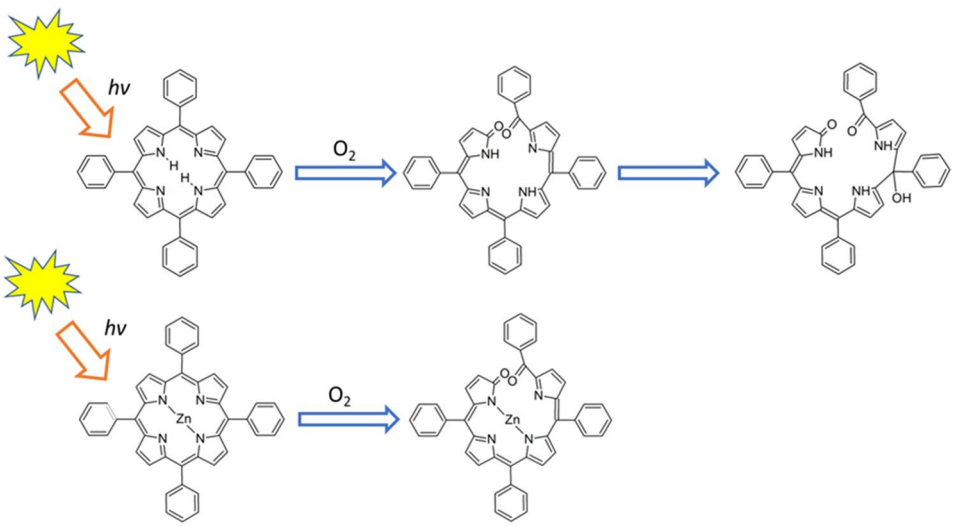

Keywords Photostability · Photooxidation · Porphyrins · Biladienones

Extended author information available on the last page of the article

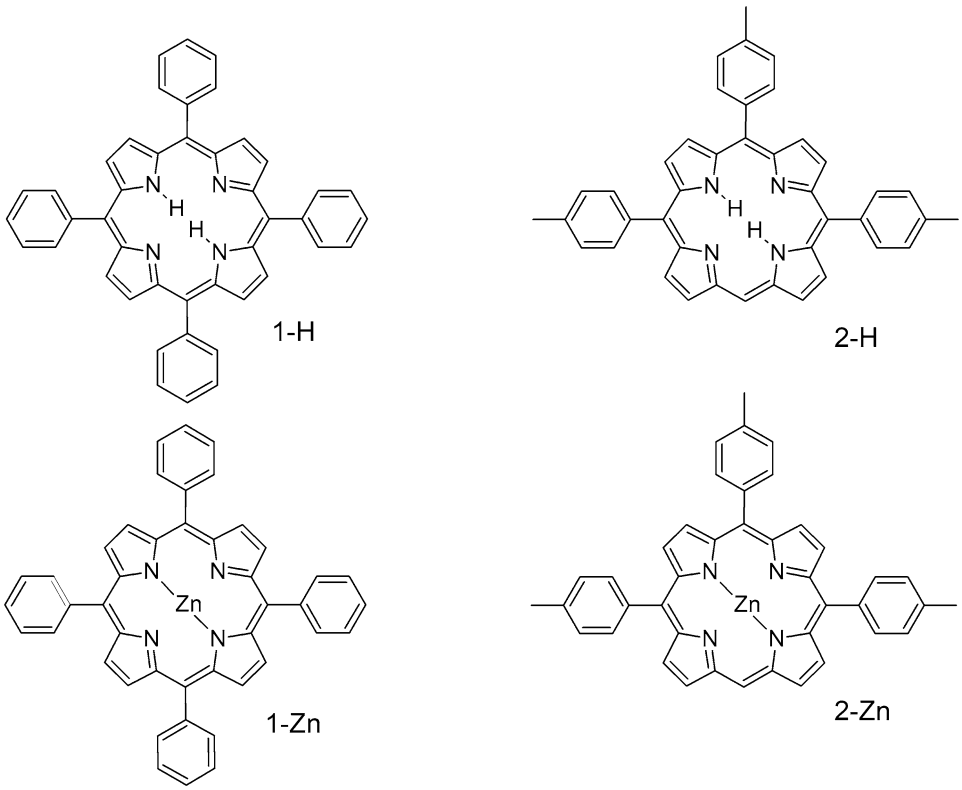

Scheme 1. The investigated porphyrins: 5,10,15,20-tetraphenylporphyrin (1-H), 5,10,15-tri(*p*-tolyl) porphyrin (2-H), zinc 5,10,15,20-tetraphenylporphyrin (1-Zn) and zinc 5,10,15-tri(*p*-tolyl) porphyrin (2-Zn)

1 Introduction

The photostability of a chromophore is a crucial factor for rational design of systems that are considered for applications in the areas that involve light-matter interactions, such as photovoltaics, display panels, dyes for fluorescence imaging, photodynamic therapy, etc. Porphyrins—justly called "pigments of life" [1]—are quite often used in these fields; in particular, they are the main photosensitizers exploited in the photodynamic therapy of cancer, skin diseases or photoinactivation of bacteria. Since these modalities are based on the interaction with oxygen, an obvious question is how the presence (or absence) of oxygen affects the photodegradation quantum yield. Numerous papers have been devoted to the photochemistry of porphyrinoids [2–20], but the role of oxygen is still under debate. The review by Bonnet and Martinez [5] mentions that the removal of oxygen usually improves photostability, but the opposite behavior has also been reported. Our recent works were aimed at enhancing the photostability by quenching the porphyrin triplet state with cyclooctatetraene (COT) covalently attached to the porphyrin macrocycle [21, 22]. This strategy worked very well for oxygen-free solutions, but the results obtained in the presence of oxygen were more complex: improvement of photostability was observed for COT-functionalized zinc porphyrins, whereas their free base analogues were found to be less stable. These studies suggested that photodegradation can proceed along different paths for oxygenated and deaerated solutions.

The structure of the products of light-induced or chemical oxidation as well as the reaction mechanisms were extensively discussed for *meso*-tetraphenylporphyrin in its free base, metalated, and anionic forms [8–11, 14–16, 23, 24]. In particular, by combining NMR, mass spectroscopy, and isotope substitution, Cavaleiro and coworkers were able to propose a violinoid rather than biliverdinoid structure of the oxygen-containing products [9, 10, 23].

In the present work, we study the photobleaching of free base and zinc forms of two porphyrins, substituted at the *meso* positions with four phenyl or three tolyl groups (Scheme 1). The main goals were (i) to identify the products of photoinduced decomposition, (ii) to compare the photochemistry in degassed and non-degassed solutions, and (iii) to understand the differences between photodestruction mechanisms of free base and zinc porphyrins.

2 Experimental

Commercially available sample of 1-H (HPLC grade, SIGMA) has been used. 1-Zn was produced in our laboratory and checked for purity by spectroscopic methods. 2-H

and 2-Zn were obtained as described previously [21]. The following solvents (spectroscopic or LCMS grade, Merck) have been used in these studies: toluene, dimethyl sulfoxide (DMSO), methanol, and water.

Electronic absorption spectra were measured using a Shimadzu UV 2700 spectrophotometer.

For irradiation of the samples (placed in quartz cuvettes), two different Thorlabs high power LEDs have been used: SOLIS-405C (measured maximum at 409 nm, 432 mW) and M420L2 (420 nm, 11, 47, 63, or 170 mW).

The photobleaching quantum yield (Φ_{pb}) has been determined by measuring the sample absorbance before irradiation (A_0) and at time t after the beginning of irradiation ($A(t)$). The $A_0/A(t)$ ratio was plotted as a function of $F(t)$, defined as $N_{tot}(t)/A(t)$, where $N_{tot}(t)$ denotes the total number of photons absorbed after irradiating the sample for time t (Figs. S5–S8). It can be shown that $\Phi_{pb} = (b \times N_{Av} \times V)/(1000 \times \varepsilon \times l)$; b is the slope in the equation: $A_0/A(t) = 1 + bF(t)$, N_{Av} is the Avogadro number, V is the sample volume (in mL), ε is the molar absorption coefficient at the wavelength selected to monitor absorbance decrease, and l is the optical path length (in cm). Further details can be found elsewhere [22]. We estimate that the error in the obtained Φ_{pb} value does not exceed 30%.

The triplet state lifetimes were measured using a home-built setup for transient absorption measurement in nano- to milliseconds time domains. An Opotek Radiant 355 laser (210–2500 nm tuning spectral region, 5 ns pulsewidth, 10 Hz repetition rate) was used as the excitation source. All compounds were excited in the region of the Soret band (400–430 nm, the pulse energy was in the range of 30–200 µJ). The continuous output of a laser-driven Xe lamp (Energetiq EQ-99-Plus-EU) was used as a probe light source. The setup was equipped with a Hamamatsu R955 photomultiplier and a Yokogawa (Tokyo, Japan) DL9140 fast oscilloscope. The samples were deaerated before measurements by a freeze–pump–thaw method. At least seven freeze–pump–thaw cycles were done before each lifetime experiment. The last pumping cycle was done at the pressure of 2×10^{-5} mbar. To check the quality of deoxygenation, two additional freeze–pump–thaw cycles were done after lifetime measurements and the experiment was repeated. The difference in the obtained lifetimes was near 0.4%, which is lower than the estimated experimental error (1–2%). A low concentration of the investigated compounds, close to 10^{-6} M, was used to avoid triplet–triplet annihilation. One should note that under these conditions, the concentrations of porphyrin and of the oxygen remaining in the sample after degassing, can be comparable, as estimated from the triplet lifetimes of porphyrins in degassed and non-degassed solutions.

Mass spectroscopy experiments have been performed on Shimadzu Nexara X2 LC/MS/MS 8050 system with positive and negative ESI ionization methods. The samples dissolved in toluene (concentration of about 5×10^{-6} mol dm^{-3}) before and after irradiation were transferred into UPLC vials and subsequently injected into the LC/MS/MS system for the determination of the masses of the substrate and the photoproducts. Chromatographic separation was achieved with a Kinetex 2.6 µm XB-C18 100 Å, LC column 100 × 2.1 mm (Phenomenex). The ESI–MS settings were as follows: capillary voltage 4000 V (positive mode) and 3000 V (negative mode), nebulizing gas flow 3.0 L/min, and drying gas flow 5 L/min at 300 °C. The column temperature was set at 40 °C. The mass-to-charge ratio (m/z) scan range was from 150 to 850 (positive and negative). The mobile phase was composed of methanol (90%) and water (10%). The flow rate was 0.4 mL/min with an isocratic elution. The injection volume was 1 µL. For the processing of the data, LabSolutions software (Shimadzu) was used.

Quantum chemical calculations were done using version 2022.103 of the Amsterdam Density Functional (ADF) package [25]. BP86-D functional was chosen, combined with DZP basis set. Before performing TD-DFT simulations of electronic transitions, the geometry was optimized, and the Hessian was checked to see if all the calculated vibrational frequencies are positive.

3 Results

Irradiated solutions of porphyrins in toluene reveal changes in absorption, indicating photodecomposition (Fig. 1). 1-H and 2-H behave very similarly (Fig. 1). Absorption decreases, and no apparent spectral features are observed that could be assigned to photoproducts. However, closer inspection of the spectra reveals the presence of new bands, much weaker in intensity than those of the substrate. They could be visualized by subtracting the contribution of the substrate (Fig. 1, bottom). At the beginning of irradiation, a broad band appears, peaking at 607 and 595 nm in 1-H and 2-H, respectively. It shifts with time to 554 nm in 1-H; in 2-H, two peaks are observed at 547 and 525 nm. In both molecules, another band with the maximum around 325 nm grows with irradiation. Its position does not change with time.

The situation is different for degassed solutions, as illustrated for 2-H in Fig. 2. Practically no new bands are observed, except for a 325 nm feature, much less intense than observed in non-degassed solutions. We cannot definitely exclude that it is due to remaining traces of oxygen.

One immediately notices a large decrease in photostability when the sample is deoxygenated. The whole population of 2-H disappeared after 10 h of irradiation (Fig. 2). In degassed toluene, the photobleaching quantum yield is an

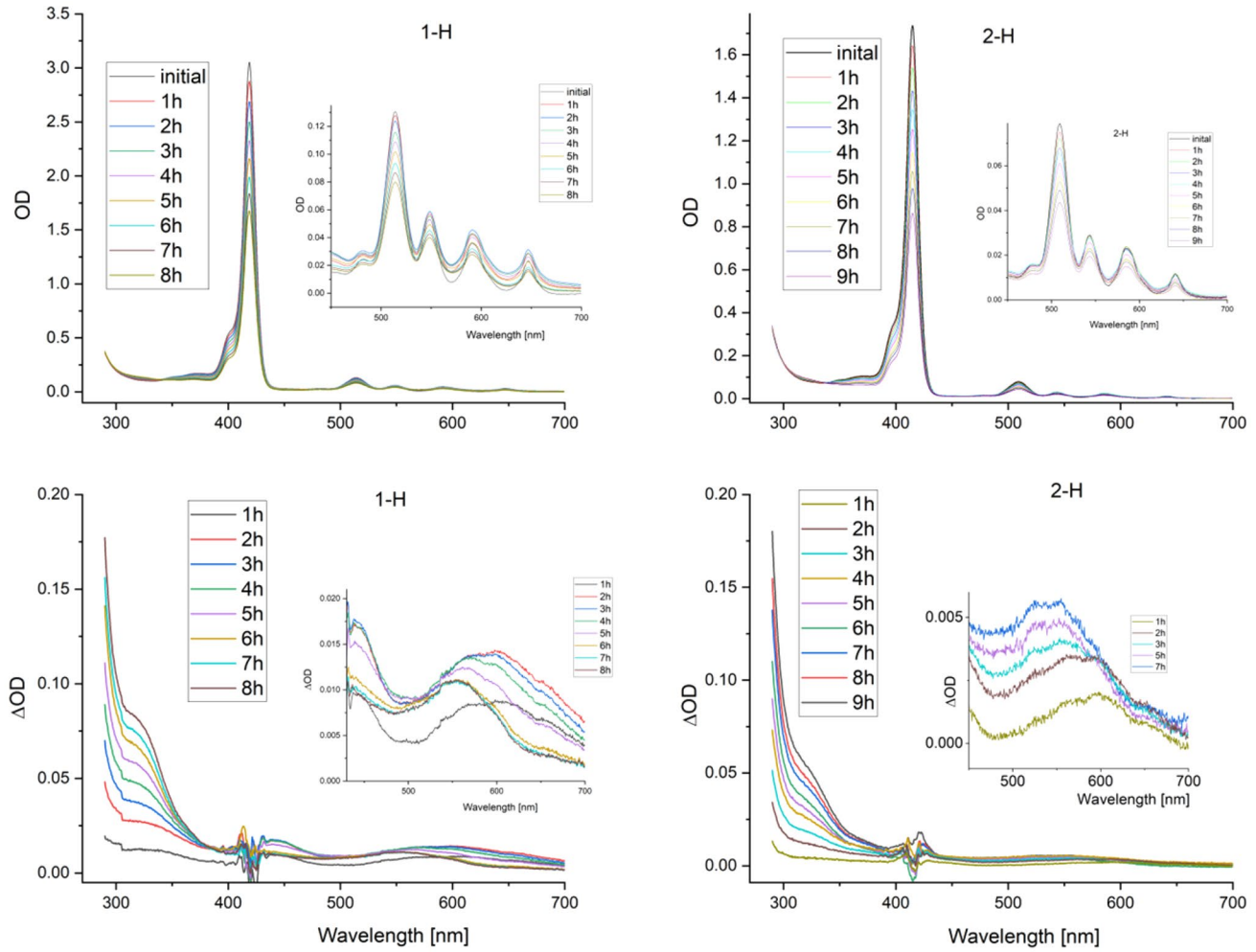

Fig. 1 Monitoring photodegradation of 1-H (left) and 2-H (right) in non-degassed toluene. Samples were irradiated with an LED (409 nm maximum, power of 432 mW). Top, changes in the absorption spectra. Bottom, absorption spectra obtained after subtracting the contribution from the substrate

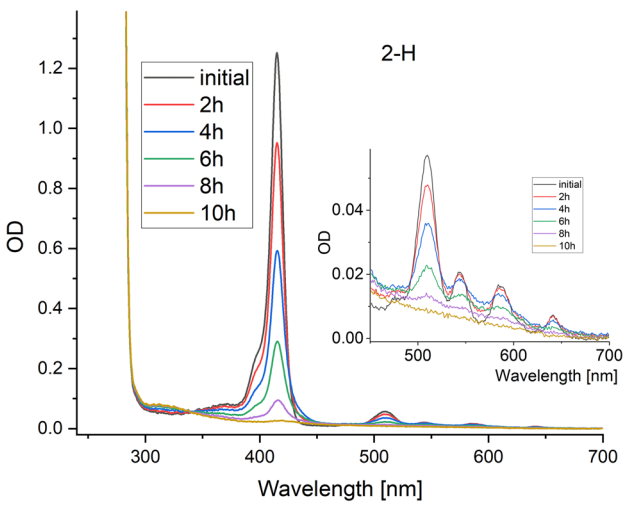

Fig. 2 Monitoring photodegradation of 2-H in degassed toluene. Irradiation with 420 nm LED, 63 mW power

order of magnitude higher than in the non-degassed solvent (Table 1).

Both zinc porphyrins exhibit similar photochemistry, which, at first glance, seems to be very different from the behavior of free bases. Changes in absorption are so distinct that no special procedures are required for the visualization of the new bands formed after irradiation (Fig. 3). The decrease of the initial absorption is accompanied by a rise of new bands at 630, 490 (1-Zn) or 480 and at *ca*. 350 nm (2-Zn). In contrast to the situation in free bases, very similar pattern of absorption changes is observed for zinc derivatives in oxygen-containing and deoxygenated solutions. However, photodegradation proceeds much faster in the degassed solutions. For instance, for similar initial absorption and irradiation conditions, 2-Zn is destroyed in about two hours in non-deaerated toluene, whereas, after degassing, the same process takes about 10 min (*cf*. Figure 3, middle and bottom parts).

Table 1 Quantum yields of photodegradation

Compound	Non-degassed toluene[a]	Deaerated toluene
1-H	2.6×10^{-7} (170 mW, 420 nm) 2.5×10^{-7} (47 mW, 420 nm)	2.0×10^{-6} (170 mW, 420 nm) 2.7×10^{-6} (47 mW, 420 nm)
1-Zn	8.1×10^{-6} (11 mW, 420 nm)	3.8×10^{-4} (11 mW, 420 nm)
1-Zn-DMSO complex	2.1×10^{-6} (170 mW, 420 nm)	3.7×10^{-5} (170 mW, 420 nm)
2-H	2.2×10^{-7} (63 mW, 420 nm) 2.2×10^{-7} (432 mW, 409 nm)	3.3×10^{-6} (63 mW, 420 nm)
2-Zn	2.5×10^{-5} (63 mW, 420 nm)	4.8×10^{-4} (63 mW, 420 nm)

[a]Estimated error: ± 30%

LC–MS spectra were obtained for samples that were irradiated for a certain period of time (1-H: 14 h, 2-H: 15 h, 1-Zn: 45 min, 2-Zn: 1 h; irradiated with 432 mW 409 nm LED). In the spectra obtained after photodegradation of both zinc porphyrins (Figs. S2 and S4), the dominant peak corresponded to the mass larger than in the initial compound by 32, clearly suggesting the attachment of two oxygen atoms. Interestingly, the analogous peaks were not present in the positive MS spectra of the photodecomposition products of free bases. Instead, several peaks corresponding to lower mass were observed: 320, 276, and 93 for 1-H (Fig. S1) and 304, 326, 348, 415, 437, and 453 for 2-H (Fig. S3).

The irradiation of the degassed 1-Zn sample (50 s, 420 nm, 170 mW) leads to the formation of the product with the mass larger by 32 from the mass of substrate. This suggests that this product also contains two oxygen atoms in the structure. A possible explanation for this observation is that 1-Zn forms a complex with remaining oxygen or oxygen-containing species, which is not dissociated under the degassing procedure. To check this hypothesis, we performed an additional experiment in which DMSO (20 µL) was added to the 1-Zn toluene solution (3 mL). Dimethyl sulfoxide is known to form complex with 1-Zn [26]; it can therefore be expected to replace oxygen or water bound to zinc. For the non-degassed sample of the solution of 1-Zn containing DMSO (irradiated for 90 min with 170 mW, 420 nm LED), the MS spectra have shown that the oxygenated product with the mass larger by 32 than the mass of 1-Zn still forms. In contrast, in the degassed sample (170 mW, 420 nm, 6 min irradiation) this product was not present. In addition to lower masses (347 and 240), which demonstrate porphyrin fragmentation, a mass of 767 was detected, strongly suggesting an adduct with toluene. However, since the amount of the photoproduct was too small to measure NMR, we are not able to determine the exact structure.

4 Discussion

The combined results of absorption and LC–MS studies can be summarized as follows:

- Photostability of all the investigated porphyrins is significantly lower in the degassed solutions
- Zinc porphyrins are much less photostable than their free base analogues

We first discuss the results obtained for "normal", non-degassed solutions. There is little doubt that, under these conditions, photooxidation is the dominant mechanism. The LC–MS spectra show that the photoproduct contains Zn and two oxygen atoms. On the basis of absorption spectrum, its structure can be readily assigned to the dehydrated form of zinc biladienone (Scheme 2). This species, with the absorption maximum around 480 nm, has been referred to in the literature as "yellow–brown complex" [23, 27] which can coexist with the hydrated form, dubbed "blue complex", characterized by absorption at 584 and 630 nm. [27, 28] The population ratio between the two forms depends on solvent and temperature. A controversy exists in the literature regarding the relative stabilities. For the same solvent, chloroform, it was reported that the yellow–brown complex converts to the blue one [23], whereas another paper [27] claimed that the dehydrated form is more stable. Our results obtained for toluene solution support the latter (Table 2).

Interestingly, for photooxidation of magnesium *meso*-tetraphenyl porphyrin, carried out in dichloromethane, the dehydrated structure was postulated to be an intermediate, undergoing transformation into metal-free benzoylbilitriene [15]. Different behavior in toluene compared with dichloromethane may be explained by the fact that photoirradiation of porphyrins in the latter leads to acidification of the solvent [29–33]. This may accelerate the demetallation process in dichloromethane. We also note that the absorption spectrum previously assigned to the hydrated form of zinc biladienone [15] contains a weak absorption band at ~ 470 nm and the strongest peak at 628 nm. We see analogous peaks in toluene at 490 and 628 nm (Fig. 3), but the intensity ratio is reversed: the 490 nm band is much stronger than the one at 628 nm; in the spectrum shown in ref [15] the opposite ratio was observed. This leads to the conclusion that while the 470 nm band is due to metallated species, dominant in toluene, in dichloromethane only a small fraction of metal-containing

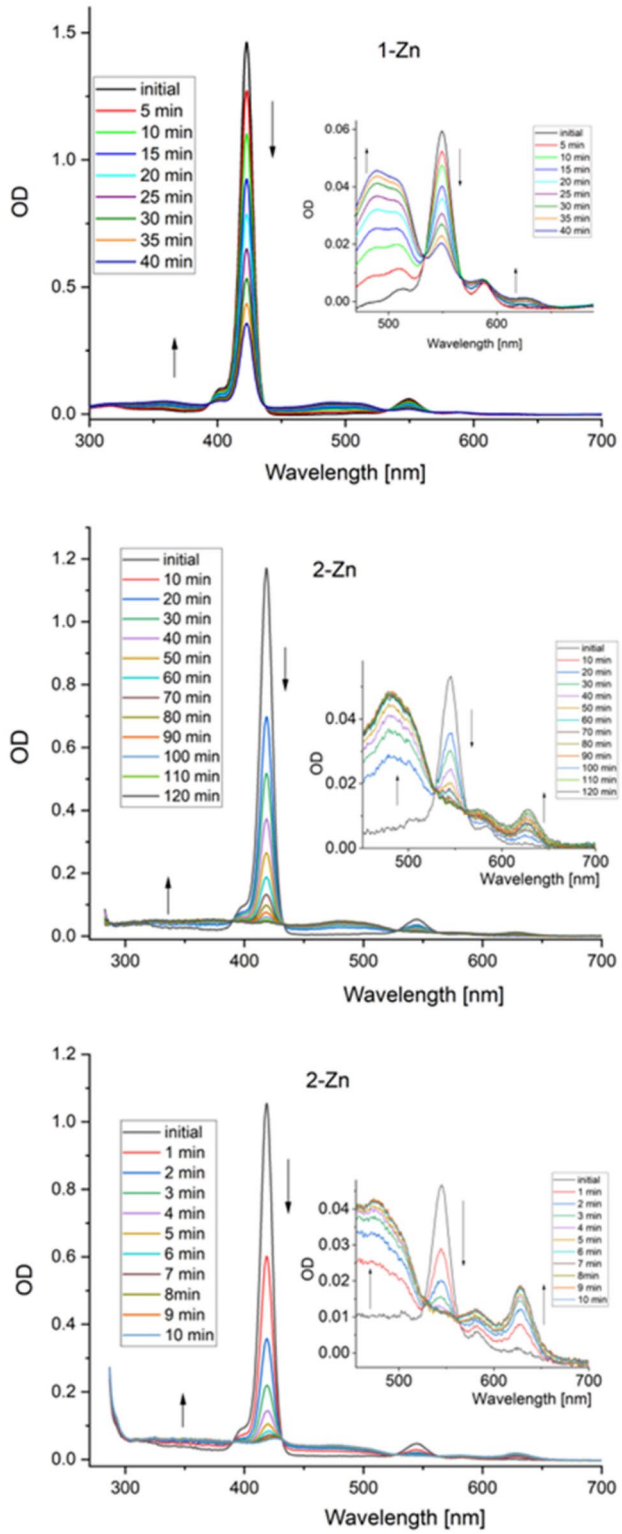

Fig. 3 Monitoring photodegradation of 1-Zn (top) and 2-Zn (middle) in non-degassed and of 2-Zn (bottom) in degassed toluene. Irradiation with 420 nm LED, 63 mW power

porphyrin remains, and the absorption at 628 nm corresponds to metal-free benzoylbilitriene, perhaps with a contribution from the hydrated form of zinc biladienone.

For the molecules presented in Scheme 2, various conformeric forms are possible. We simulated the absorption spectrum (Fig. 4) for the structure that was found as a real minimum in the geometry optimization procedure. It qualitatively agrees with experiment (*cf.* Fig. 3) regarding both spectral shifts and significantly decreased absorption intensity.

For both 1-H and 2-H, two products are observed, characterized by the absorption maxima around 600 and 550 nm, respectively. The absorption of the latter is similar to the spectra reported for the free base analogues of the hydrated zinc biladienone species. Since the 600 nm species appears earlier on, it seems reasonable to assign it to the dehydrated structure, obtained after attachment of an oxygen molecule. The difference in stability between the zinc dehydrated form and the readily hydrated free base can be explained by the lack of central metal ion in the former. The source of hydration is water present in spectral toluene at concentration much higher than that of the porphyrin substrate.

One can conclude that in both free base and zinc derivatives the initial step of photodegradation involves the same, well-known mechanism: oxidative ring opening by molecular oxygen. In free bases, this is followed by hydration, whereas the dehydrated form of zinc biladienone is stable.

Using the absorption coefficients of the hydrated free base and dehydrated zinc biladienones [27] (reported for porphyrins bearing dodecyloxy groups in the *para* position of phenyl substituents), it was possible to make a rough estimation of photoconversion efficiency. For the zinc derivatives, a value of 39% was obtained in the initial stages of irradiation (after 20 min). When the whole substrate was photolyzed, this value dropped to 34%, indicating partial photodegradation of biladienone. The same procedure applied to free bases yielded the values of about 20%, consistent with the finding that the photoconversion products were more easily observed in the zinc derivatives (another factor is a larger absorption coefficient in the zinc biladienones).

Spectral changes in absorption of 1-H and 2-H that accompany irradiation of samples in degassed toluene are different than in the case of oxygen-containing solvent. As could be expected, the 600 and 550 nm bands assigned to oxidized species are not present. Instead, growth of absorption is observed at the red edge of the Soret band, around 435 nm. After the initial increase, the absorption at this wavelength becomes lower. This indicates that the primary photoproduct is efficiently photobleached. We cannot assign the structure, but a small spectral separation of 435 nm and the maximum of the Soret band in 1-H and 2-H suggests that the porphyrin macrocycle is retained. On the other hand, the products of degradation of the initially formed species most

Scheme 2. Dehydrated (**a**) and hydrated (**b**) structures of the photooxidation products

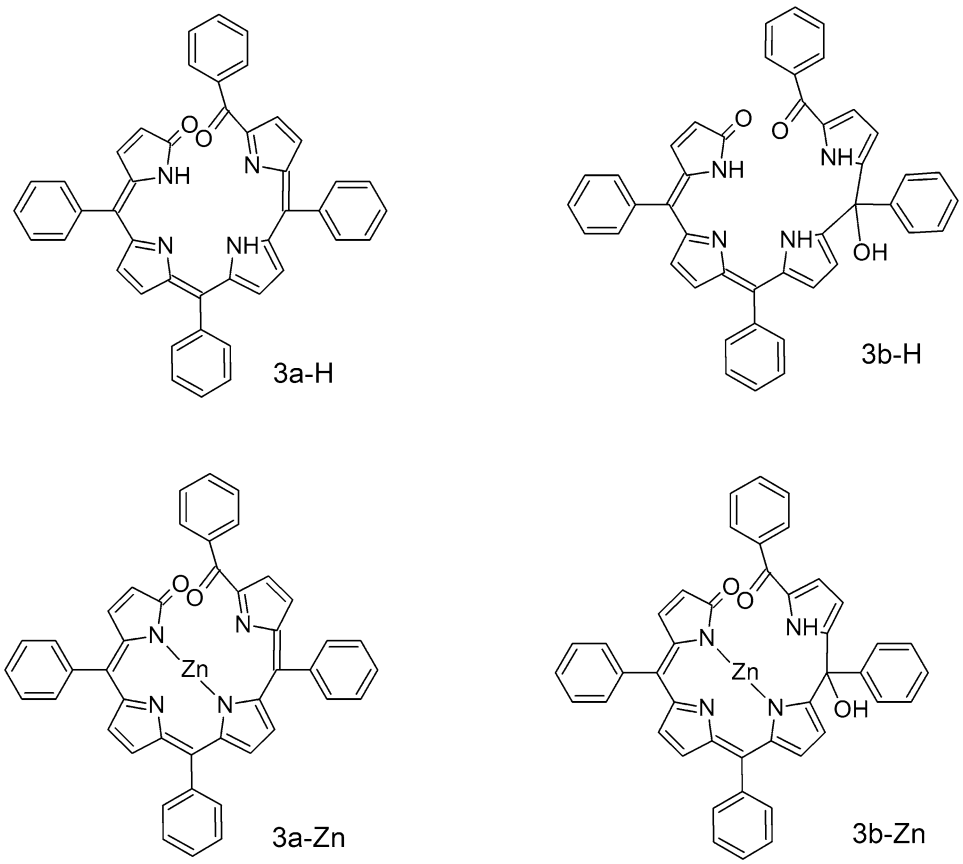

Table 2 Triplet lifetimes

Compound	Non-degassed toluene [ns][a]	Deaerated toluene [μs]
1-H	196	286
1-Zn	309	310
1-Zn:DMSO	707	616
2-H	247	207
2-Zn	362	266

[a]Estimated error: ± 2%

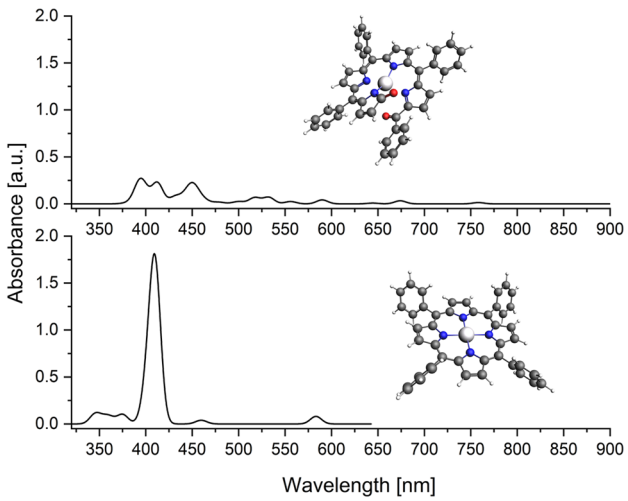

Fig. 4 Simulated absorption spectra of 1-Zn (bottom) and of the postulated photooxidation product (top)

probably correspond to smaller fragments, responsible for the constant growth of absorption at 320 and below 290 nm.

A surprising result was obtained while monitoring photoconversion of both zinc porphyrins in degassed solutions (Fig. 3). Changes in absorption were very similar to those observed for oxygen-containing solvents. The formation of the same product as in the latter was also confirmed by MS data. We are rather certain that the degassing was carried out properly; this was confirmed by the long triplet lifetimes, remaining practically the same after several freeze–thaw cycles. The formation of an oxygen-containing product can be explained by a reaction with remaining oxygen or other oxygen-containing species. A paper exists describing coordination of oxygen donor ligands to 1-Zn [26]. Interaction of zinc porphyrin with O_2 has also been studied theoretically [34]. Formation of complexes with molecular oxygen seems improbable, as the triplet lifetime of such species is expected to be much shorter than the values obtained for

degassed toluene solutions. At present, water seems to be the most plausible candidate for the complexing agent.

The hypothesis of the presence of oxygen-containing complexes was confirmed by studying photodegradation in toluene solutions containing dimethyl sulfoxide, which is known to efficiently complex 1-Zn [26]. The results are shown in Fig. 5. For non-degassed solutions, changes in absorption are similar to those observed for pure toluene (cf. Fig. 3), indicating formation of the same product. We note an increase in photostability: photodegradation quantum yield decreases by the factor of four.

In degassed solutions containing 1-Zn:DMSO complex the photostability increases by an order of magnitude. Most importantly, absorption changes are now very different from those observed in pure toluene solutions. In particular, absorption in the 800–900 nm region, characteristic of 3a-Zn and observed in non-degassed solution, disappears upon deoxygenation. We conclude that complexation by DMSO is an efficient way of protecting against oxygen and that the irradiation now leads to a different photoproduct. In fact, for degassed solutions, the absorption changes in DMSO-complexed zinc porphyrins now resemble those observed in free bases: the largest absorption growth occurs at 457 nm, whereas for free bases increase was observed around 440 nm (cf. Fig. 2).

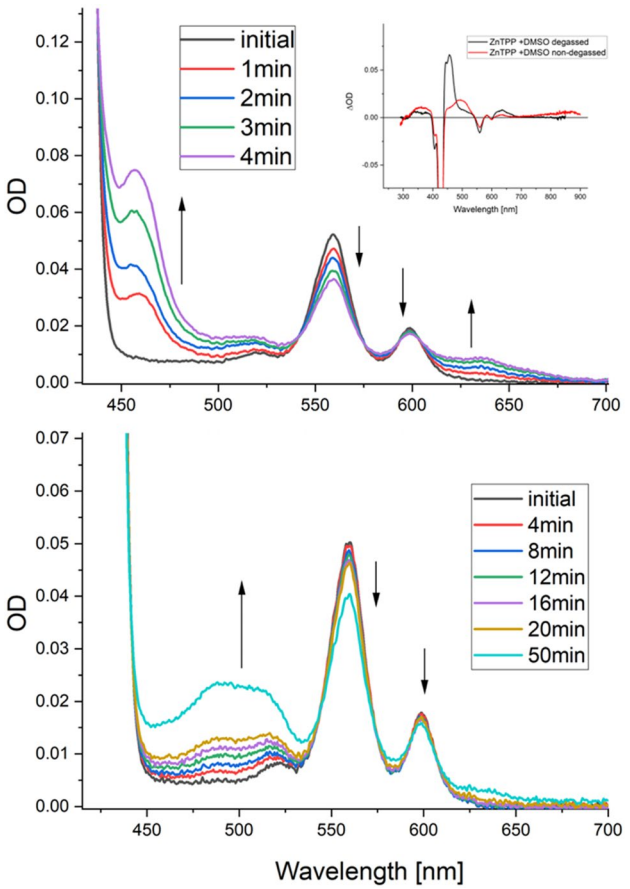

Fig. 5 Absorption changes observed for 1-Zn in toluene solutions containing 10^{-1} M DMSO. Bottom, non-degassed, top, degassed solution. Irradiation with 420 LED, 170 mW power. Inset, comparison of absorption changes recorded for degassed (black) and non-degassed (red) solutions

It should be noted that our values of photobleaching quantum yield of 1-H are considerably lower than those previously reported for the same compound in the same solvent [11]. Several factors may be responsible for this difference. Some of them may be related to somewhat different experimental parameters, such as spatial profile of irradiation and/or stirring of the solution. One cannot exclude, however, that the different irradiation conditions may alter the contributions from different photodegradation channels, because the previous data were obtained using much stronger light sources. We looked for the possibility of irradiation power dependence of the photodegradation quantum yield. The results obtained when irradiating into the Soret band indicate that there is no power dependence, but this does not exclude such dependence for other wavelengths. It would be very useful to establish detailed protocols and standards for accurate measurements of photobleaching quantum yield, analogous, e.g., to the IUPAC technical report on photoluminescence quantum yield measurements by Brouwer [35].

Using the values of photodestruction quantum yields and triplet lifetimes, and assuming that photodegradation occurs from the triplet state, one can determine k_{pb}, the rate of photobleaching, using the formula: $k_{pb} = \Phi_{pb}/(\Phi_T \times \tau_T)$; τ_T is the triplet lifetime and Φ_T is the triplet formation yield. Setting $\Phi_T = 0.80$ for free bases and 0.88 for zinc porphyrins [36], yields the rates shown in Table 3. These values immediately show that the lower photostability in deaerated solution is not due to larger k_{pb}. In fact, the rate becomes smaller in the absence of oxygen, but, because the triplet lifetime increases by three orders of magnitude, the photostability decreases. This finding demonstrates a well-known dual role of oxygen as (i) a triplet quencher and (ii) oxidating agent. These two factors act in opposite directions regarding photostability. For the presently studied porphyrins, the triplet quenching ability of oxygen wins over its oxidative power.

Table 3 Photodegradation rates

Compound	Non-degassed toluene [s^{-1}]	Deaerated toluene [s^{-1}]
1-H	1.59	0.012
1-Zn	29.8	1.39
1-Zn:DMSO	3.38	0.068
2-H	1.11	0.020
2-Zn	78.5	5.98

5 Summary

Our results indicate that the initial photodestruction channel is the same in free bases and zinc porphyrins: attachment of the oxygen molecule, formed by the rupture of C(*meso*)-C(α) bond and formation of biladienone 3a. This photoproduct remains stable in zinc porphyrins, due to stabilization by coordinated metal, but in free bases it is converted to the hydrated form 3b.

Photodegradation of porphyrins provides an example of a specific photochemical kinetics, where more efficient substrate decomposition does not imply a larger reaction rate, but the longer lifetime of the precursor: the molecule in the triplet state.

The structure of the photoproducts obtained in the degassed solutions remains to be determined. Since the photoproducts reveal the strongest absorption in the region of the Soret band, one can assume that porphyrin skeleton is preserved, modified by attachment of the solvent molecule (as indicated by MS for 1-Zn) or an impurity, such as water.

Finally, we note a protective role of DMSO complexation in enhancing photostability. This effect is particularly strong for deaerated solutions. It is remarkable that the twofold lengthening of the triplet lifetime in the complex, which acts towards increasing the photobleaching yield is more than counterbalanced by the 20-fold decrease in the degradation rate. The situation is similar for non-degassed solutions, although now the rate decrease is somewhat smaller (sevenfold). Thus, in both cases, zinc porphyrin becomes more photostable upon forming a complex with DMSO.

Supplementary Information The online version contains supplementary material available at https://doi.org/10.1007/s43630-023-00482-6.

Acknowledgements This work was supported by the Polish National Science Center, grant 2016/22/A/ST4/00029, and by the grant from the PL-Grid infrastructure.

Data availability The data that support the findings of this study are available from the corresponding author upon reasonable request.

Declarations

Conflict of interest On behalf of all authors, the corresponding author states that there is no conflict of interest.

References

1. Battersby, A. R., Fookes, C. J. R., Matcham, G. W. J., & McDonald, E. (1980). Biosynthesis of the pigments of life: Formation of the macrocycle. *Nature, 285*, 17–21.
2. Wojaczyński, J. (2014). Degradation pathways for porphyrinoids. In R. Paolesse (Ed.), *Synthesis and Modifications of Porphyrinoids* (pp. 143–202). Springer, Berlin Heidelberg.
3. Wojaczynski, J., & Latos-Grazynski, L. (2010). Photooxidation of N-confused porphyrin: a route to N-confused biliverdin analogues. *Chemistry–A European Journal., 16*, 2679–2682.
4. Wojaczynski, J., Duszak, M., & Latos-Grazynski, L. (2013). Photooxidation of unhindered triarylcorroles. *Tetrahedron, 69*, 10445–10449.
5. Bonnett, R., & Martinez, G. (2001). Photobleaching of sensitisers used in photodynamic therapy. *Tetrahedron, 57*, 9513–9547.
6. Ion, R.-M. (2017). Porphyrins and phthalocyanines: photosensitizers and photocatalysts. In Y. Yusuf (Ed.), *Phthalocyanines and Some Current Applications* (p. 9). IntechOpen.
7. Harriman, A., Porter, G., & Walters, P. (1983). Photooxidation of metalloporphyrins in aqueous-solution. *Journal of the Chemical Society, Faraday Transactions, 1*(79), 1335–1350.
8. Harriman, A., Porter, G., & Searle, N. (1979). Reversible photooxidation of zinc tetraphenylporphine by benzo-1,4-quinone. *Journal of the Chemical Society, Faraday Transactions, 2*(75), 1515–1521.
9. Cavaleiro, J. A. S., Neves, M. G. P. S., Hewlins, M. J. E., & Jackson, A. H. (1990). The photooxidation of meso-tetraphenylporphyrins. *Journal of the Chemical Society, Perkin Transactions, 1*, 1937–1943.
10. Cavaleiro, J. A. S., Hewlins, M. J. E., Jackson, A. H., & Neves, G. P. M. S. (1986). Structures of the ring-opened oxidation-products from meso-tetraphenylporphyrin. *Journal of the Chemical Society, Chemical Communications, 2*, 142–144.
11. Cavaleiro, J. A. S., Gorner, H., Lacerda, P. S. S., MacDonald, J. G., Mark, G., Neves, M. G. P. M. S., Nohr, R. S., Schuchmann, H. P., van Sonntag, C., & Tome, A. C. (2001). Singlet oxygen formation and photostability of meso-tetraarylporphyrin derivatives and their copper complexes. *Journal of Photochemistry and Photobiology A: Chemistry, 144*, 131–140.
12. Fuhrhop, J. H., & Mauzeral, D. (1971). Photooxygenation of magnesium-octaethylporphin. *Photochemistry and Photobiology., 13*, 453–458.
13. Wasser, P. K. W., & Fuhrhop, J. H. (1973). Photooxygenation of metalloporphyrins and metallochlorins. *Annals of the New York Academy of Sciences, 206*, 533–548.
14. Smith, K. M., Brown, S. B., Troxler, R. F., & Lai, J. J. (1982). Photo-oxygenation of meso-tetraphenylporphyrin metal-complexes. *Photochemistry and Photobiology, 36*, 147–152.
15. Smith, K. M., Brown, S. B., Troxler, R. F., & Lai, J. J. (1980). Mechanism of photo-oxygenation of meso-tetraphenylporphyrin metal-complexes. *Tetrahedron Letters, 21*, 2763–2766.
16. Matsuura, T., Inoue, K., Ranade, A. C., & Saito, I. (1980). Photoinduced reactions. 104. Photo-oxygenation of magnesium meso-tetraphenylporphyrin. *Photochemistry and Photobiology., 31*, 23–26.
17. Krasnovskii, A. A., Jr., Venediktov, Y. A., & Chernenko, O. M. (1982). Quenching of singlet oxygen by the chlorophylls and porphyrins. *Biophysics, 27*, 1009–1016.
18. Šima, J. (1995). Photochemistry of tetrapyrrole complexes. *Structure and Bonding, 84*, 135–193.
19. Hopf, F. R., & Whitten, D. G. (1978). 6—Chemical transformations involving photoexcited porphyrins and metalloporphyrins.

In D. Dolphin (Ed.), *The Porphyrins* (pp. 161–195). Academic Press.
20. Whitten, D. G., Meyer, T. J., Hopf, F. R., Ferguson, J. A., & Brown, G. (1973). Photochemistry and redox activity of some metalloporphyrin complexes. *Annals of the New York Academy of Sciences, 206*, 516–532.
21. Ostapko, J., Gorski, A., Buczyńska, J., Golec, B., Nawara, K., Kharchenko, A., Listkowski, A., Ceborska, M., Pietrzak, M., & Waluk, J. (2020). Towards more photostable, brighter, and less phototoxic chromophores: synthesis and properties of porphyrins functionalized with cyclooctatetraene. *Chemistry A European Journal, 26*, 16666–16675.
22. Buczyńska, J., Gajewska, A., Gorski, A., Golec, B., Nawara, K., Rybakiewicz, R., & Waluk, J. (2021). Synthesis and photostability of cyclooctatetraene-substituted free base porphyrins. *Chemistry-Basel, 3*, 104–115.
23. Cavaleiro, J. A. S., Hewlins, M. J. E., Jackson, A. H., & Neves, G. P. M. S. (1992). Structures of the zinc complexes of the bilinones formed by photo-oxidations of *meso*-tetraphenylporphyrins. *Tetrahedron Letters, 33*, 6871–6874.
24. Silva, A. M. S., Neves, M. G. P. M. S., Martins, R. R. L., Cavaleiro, J. A. S., Boschi, T., & Tagliatesta, P. (1998). Photo-oxygenation of meso-tetraphenylporphyrin derivatives: the influence of the substitution pattern and characterization of the reaction products. *Journal of Porphyrins and Phthalocyanines, 2*, 45–51.
25. te Velde, G., Bickelhaupt, F. M., Baerends, E. J., Fonseca Guerra, C., van Gisbergen, S. J. A., Snijders, J. G., & Ziegler, T. (2001). Chemistry with Adf. *Journal of Computational Chemistry, 22*, 931–967.
26. Nardo, J. V., & Dawson, J. H. (1986). Spectroscopic evidence for the coordination of oxygen donor ligands to tetraphenylporphinatozinc. *Inorganica Chimica Acta, 123*, 9–13.
27. Kita, K., Tokuoka, T., Monno, E., Yagi, S., Nakazumi, H., & Mizutani, T. (2006). Thermochromic and solvatochromic zinc biladienones: Dynamic equilibria of a metal complex having a flexible framework sensitive to environment. *Tetrahedron Letters, 47*, 1533–1536.
28. Akasaka, H., Yukutake, H., Nagata, Y., Funabiki, T., Mizutani, T., Takagi, H., Fukushima, Y., Juneja, L. R., Nanbu, H., & Kitahata, K. (2009). Selective adsorption of biladien-Ab-one and zinc biladien-Ab-one to mesoporous silica. *Microporous and Mesoporous Materials, 120*, 331–338.
29. Hur, D. Y. (2013). Solvent-dependent photoreactions of porphyrin-spiropyran dyad: Ring-opening or protonation. *Bulletin of the Korean Chemical Society, 34*, 3125–3128.
30. Nakano, T., & Mori, Y. (1994). Photochemical reaction in chlorinated solvents in the presence of halogenated P-benzoquinones. I. Photochemically induced acidification of solution and protonation on octaethylporphyrin in dichloromethane or chloroform. *Bulletin of the Chemical Society of Japan., 67*, 2627–2633.
31. De Luca, G., Pollicino, G., Romeo, A., Patanè, S., & Scolaro, L. M. (2006). Control over the optical and morphological properties of UV-deposited porphyrin structures. *Chemistry of Materials, 18*, 5429–5436.
32. Scolaro, L. M., Romeo, A., Castriciano, M. A., De Luca, G., Patanè, S., & Micali, N. (2003). Porphyrin deposition induced by UV irradiation. *Journal of the American Chemical Society, 125*, 2040–2041.
33. Makarska-Bialokoz, M., & Gladysz-Plaska, A. (2016). Spectroscopic analysis of porphyrin compounds irradiated with visible light in chloroform with addition of B-myrcene. *Journal of Molecular Structure, 1125*, 103–112.
34. Rusydi, F., Agusta, M. K., Saputro, A. G., & Kasai, H. (2012). A first principles study on zinc-porphyrin interaction with O-2 in zinc-porphyrin(oxygen) complex. *Journal of the Physical Society of Japan., 81*, 124301.
35. Brouwer, A. M. (2011). Standards for photoluminescence quantum yield measurements in solution (IUPAC technical report). *Pure and Applied Chemistry, 83*, 2213–2228.
36. Magdaong, N. C. M., Taniguchi, M., Diers, J. R., Niedzwiedzki, D. M., Kirmaier, C., Lindsey, J. S., Bocian, D. F., & Holten, D. (2020). Photophysical properties and electronic structure of zinc(II) porphyrins bearing 0–4 meso-phenyl substituents: zinc porphine to zinc tetraphenylporphyrin (ZnTPP). *Journal of Physical Chemistry A, 124*, 7776–7794.

Authors and Affiliations

Barbara Golec[1,2] · Joanna Buczyńska[2] · Krzysztof Nawara[1,2] · Aleksander Gorski[2] · Jacek Waluk[1,2]

✉ Jacek Waluk
jwaluk@ichf.edu.pl

[1] Faculty of Mathematics and Science, Cardinal Stefan Wyszyński University, Dewajtis 5, 01-815 Warsaw, Poland

[2] Institute of Physical Chemistry, Polish Academy of Sciences, Kasprzaka 44/52, 01-224 Warsaw, Poland